Oscillatory patterns in angular differential ion-atom charge exchange cross sections: The role of electron saddle swaps

S. Otranto, I. Blank, R. E. Olson, and R. Hoekstra

Citation: AIP Conf. Proc. **1525**, 27 (2013); doi: 10.1063/1.4802283

View online: http://dx.doi.org/10.1063/1.4802283

View Table of Contents: http://proceedings.aip.org/dbt/dbt.jsp?KEY=APCPCS&Volume=1525&Issue=1

Published by the American Institute of Physics.

Oscillatory Patterns In Angular Differential Ion-Atom Charge Exchange Cross Sections: The Role Of Electron Saddle Swaps

S. Otranto[1], I. Blank[2], R. E. Olson[3] and R. Hoekstra[2]

[1]*IFISUR and Departamento de Física, Universidad Nacional del Sur, 8000 Bahía Blanca, Argentina.*
[2]*KVI Atomic Physics, Zernikelaan 25, NL-9747 AA, Groningen, The Netherlands*
[3]*Physics Department, Missouri University of Science and Technology, Rolla MO 65409, USA.*

Abstract. In this work, we have performed an experimental/theoretical study of state selective charge exchange cross sections in 1-10 keV/amu Ne^{8+} +Na(3s) collisions. Theoretical calculations provided by the classical trajectory Monte Carlo method (CTMC) are contrasted to data obtained at KVI by means of the magneto-optical trap recoil-ion momentum spectroscopy technique (MOTRIMS). We find that for electron capture to $n \leq 10$, a two-step mechanism which involves an initial electronic excitation followed by electron capture at a later stage of the collision applies. Oscillatory structures in the n-state selective capture cross sections and recoil ion transverse momentum distributions are present in the experimental data as well as in the theoretical results, and are ascribed to the number of swaps the electron undergoes across the potential energy saddle during the collision process.

Keywords: charge exchange, ion-atom collisions.
PACS: 34.70.+e

INTRODUCTION

During the last 50 years, charge exchange studies of atom-atom [1], ion-alkali [2,3] and ion-Rydberg collisions [4] at the total cross section level have systematically indicated the presence of oscillatory structures which were either interpreted as due to a region of stationary phase in the difference between the incident and outgoing channels or, in a classical picture, the number of swaps the electron undergoes across the potential saddle before it is captured by the projectile [5]. A more detailed inspection of the physical mechanisms responsible for those oscillations was experimentally prohibitive in those days while the limited computational facilities also restricted the theoretical capabilities to further refine our understanding of those collision processes at the highly differential level.

By the mid-1990s, the development of the reaction microscope [6] gave access to kinematically complete experiments and clearly expanded the potential information that could be gained from collision studies. By the year 2000, studies involving processes like state selective charge exchange, atomic photo-double-ionization and fully differential atomic single ionization, clearly showed the underlying potential of this novel technique. Such an advance also led to the development of new techniques, like the magneto-optical trap recoil-ion momentum spectroscopy (MOTRIMS) [7-9] in which a target that is laser cooled and magnetically trapped is used in the reaction microscope. By using this technique, during the last few years the KVI group succeeded in obtaining n-state selective charge exchange cross sections for ion collisions with Na(3s) and Na*(3p) [10]. These cross sections have been checked against classical trajectory Monte Carlo (CTMC) calculations and are shown to be in good agreement for the collision systems and impact energy ranges explored [11-14]. In this sense, we now have at hand all the tools needed (experimental and theoretical) for a closer inspection of the well documented oscillatory structures in charge exchange processes involving ion collisions with alkali.

In this work, we explore the Ne^{8+}+ Na(3s) collision system in the 1-10 keV/amu energy range. Our analysis is focused on charge exchange cross sections at the n-state selective level as well as transverse recoil-ion momentum distributions. Oscillatory structures are interpreted within the CTMC model in

Application of Accelerators in Research and Industry
AIP Conf. Proc. 1525, 27-31 (2013); doi: 10.1063/1.4802283

terms of electron saddle swaps across the potential saddle.

EXPERIMENTAL METHOD

Since the MOTRIMS device developed at KVI has been described elsewhere [10,14] only a brief outline will be given here. Sodium atoms are cooled and trapped in a magneto-optical trap (MOT) using a magnetic field of 20 Gauss/cm and three counter-propagating laser beams with a diameter of 20 mm each. The total light intensity is of about 100 mW. Our ion beam is collimated to 1 mm and crossed with the MOT. The resulting Na^+ ions are extracted transverse to the ion beam direction by a low electric field (< 0.5 V cm^{-1}) and their 2D position is recorded in our detector. The resolution is 0.05 a.u. in the longitudinal direction and about 0.2 a.u. for the transverse momentum spectra [15]. From the longitudinal component of the Na^+ recoil momentum, the Q-value of the collision can be deduced, and hence the product *n*-level.

THEORETICAL METHOD

The present CTMC calculations rely on the numerical evaluation of a mutually interacting three-body system. For the Na^+ core interaction with the electron and the projectile, we have used the central model potential of Garvey et al [16] where the effective charge seen by the active electron and the projectile depends on their radial distances with respect to the target core. A classical number n_c is determined from the binding energy of the captured electron relative to the projectile:

$$E_P = -\frac{Z_P^2}{2n_c^2}. \qquad (1)$$

The quantum *n*-value corresponding to the final state is then determined through the binning condition:

$$\left[(n-1)(n-1/2)n\right]^{1/3} \le n_c \le \left[(n+1)(n+1/2)n\right]^{1/3}. \qquad (2)$$

In our CTMC code, an electron swap is recorded each time the electron position vector component along the internuclear axis ($\mathbf{r}_e \cdot \mathbf{R}$) crosses the potential saddle position r_{saddle} which is a function of the internuclear distance R. Once the electron´s energy overcomes the potential barrier it can move in the field of both ions during a lapse directly determined by the impact energy and the impact parameter. For the present Garvey representation of the target, the position of the saddle can be parametrized as:

$$r_{saddle} = r_{COB} + aR^2 e^{-\lambda R} + bR^2 e^{-\gamma R}, \qquad (3)$$

with

$$r_{COB} = R/\left(\sqrt{Z_p} + 1\right), \qquad (4)$$

which is the saddle position predicted by the Classical Overbarrier model for the hydrogen target. The parameters *a* =0.56, b= 0.12, ●=1.37 and ϒ₀=0.39 represent the correction terms introduced by the short range component of the Garvey potential. In Figure 1, we compare the hydrogenic (COB) and Garvey predictions for the potential saddle position as a function of the internuclear distance R. It seems clear that for the present case the target-ion´s area of influence extends to larger distances than predicted by the standard overbarrier prediction. This is expected to be noticeable for internuclear distances R < 22 a.u., for which the short range component of the potential starts to become relevant.

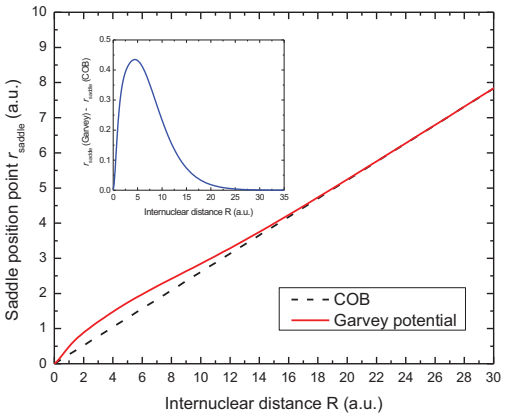

FIGURE 1. Saddle position as a function of the internuclear distance R for the standard Coulomb overbarrier prediction and the present Garvey representation of the electron-target ion interaction.

RESULTS

In Figure 2, we show state selective capture cross sections to *n* = 8-11 as a function of the impact energy in the range 1-10 keV/amu. The CTMC partial contributions arising from 1-, 3- and 5-swap contributions are explicitly shown along with the total cross section for each *n*-value. Oscillatory structures are evidenced by the experimental data in all cases and are reproduced by the present CTMC calculations.

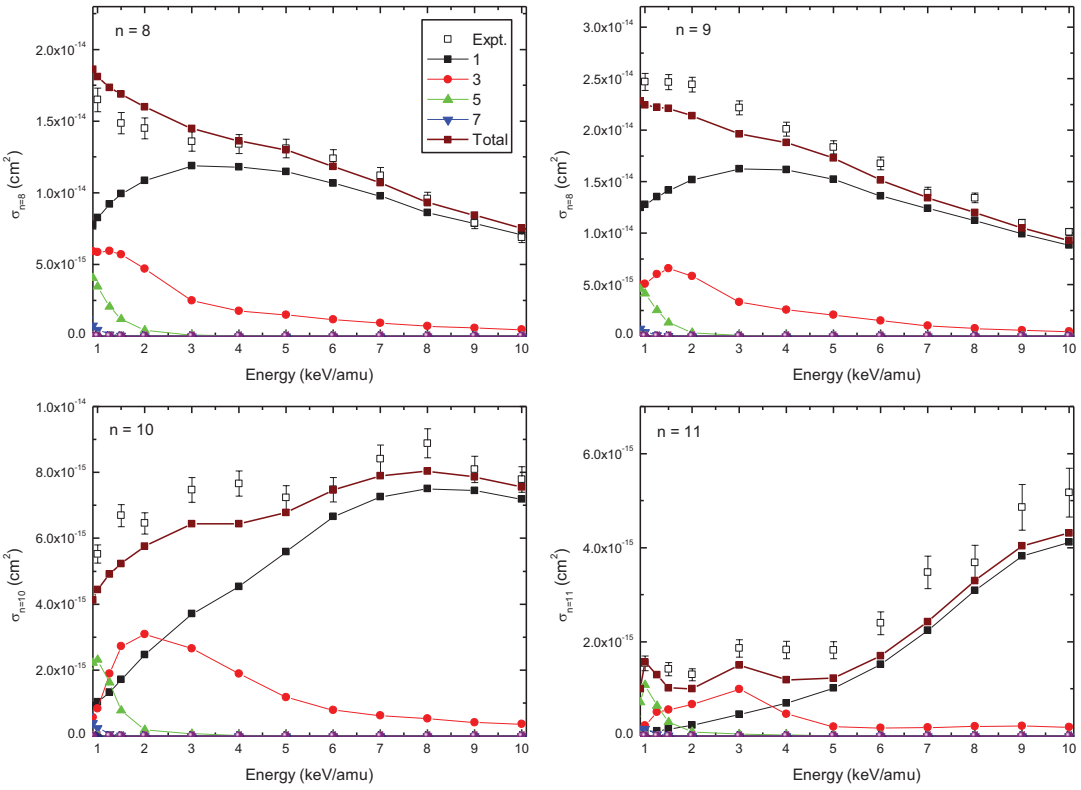

FIGURE 2. Capture cross sections to n = 8-11 for Ne^{8+} +Na(3s) collisions. The CTMC partial contributions from the different number of swaps are explicitly shown.

For energies in the order or greater than about 10 keV/amu, the 1-swap mechanism dominates and determines the energy dependence of the σ_n cross sections. As the impact energy decreases, the interaction time along with the possible number of swaps that the electron can undergo before it is finally captured increases, and as a result the relative contributions of the 3- and 5-swap mechanisms become more relevant. In this sense, in the energy range considered the CTMC results clearly highlight that the oscillatory structures in the σ_n cross sections are due to the superposition of the 1-swap and 3-swap contributions.

In Figure 3, we explore the recoil ion transverse momentum distribution for electron capture to n = 9 and 10. The collision energy in this case is 1.5 keV/amu. Clear differences among these two cases can be appreciated. While a single peak smooth structure is obtained for n = 9, a clear oscillatory structure is obtained for n = 10. From our CTMC results, we observe that the 1-, 3- and 5-swap mechanisms have different relative contributions but are nevertheless present in both n = 9 and 10. However, when these contributions are added up, and after exploring other n-values (not shown here), we conclude that for n ≤ 9 smooth 1-peak structures are obtained while oscillatory patterns are obtained for n ≥ 10. In order to understand this breakpoint in the behavior exhibited by the transverse momentum distributions for n < 10 and n ≥ 10, in Figure 4 we show the electron potential and energy-levels curves at the maximum internuclear distance at which we collect single capture events within the CTMC method. This distance, of approximately 35 a.u, is constant in the energy range considered. We note that this value is in very good agreement with the overbarrier prediction for the capture radius of 35.26 a.u.. For n = 9 and 10, the energy crossings are found at 33.8 a.u. and 53.03 a.u. respectively, indicating that capture to n ≥ 10 is only possible via the excitation of the target in an early stage of the collision process as evidenced by the energy levels of several excited states of Na which are

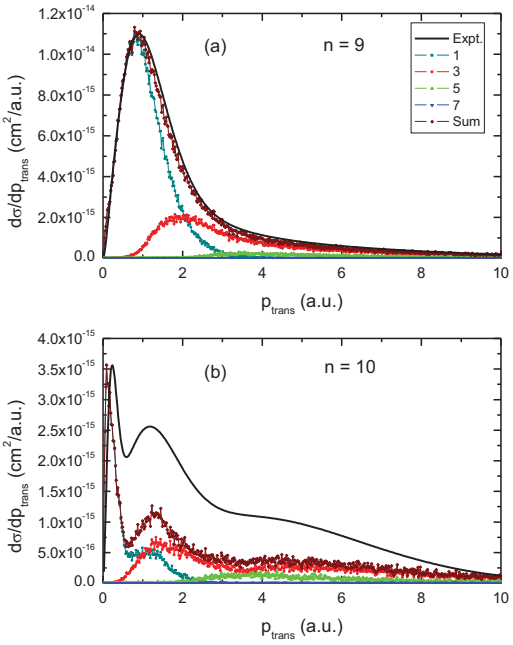

FIGURE 3. Transverse momentum distributions for 1.5 keV/amu Ne^{8+} +Na(3s) collisions leading to electron capture to (a) $n = 9$ and (b) $n = 10$. The CTMC partial contributions from the different number of swaps are explicitly shown.

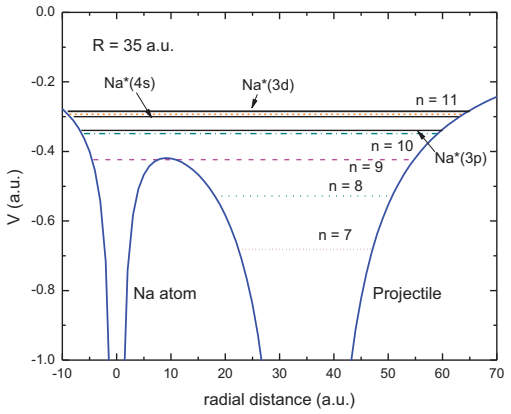

FIGURE 4. Potential and energy curves at the maximum internuclear distance for electron capture from Na(3s) (R=35 a.u.).

shown in Figure 4. Then, capture to $n \leq 10$ can take place via a two-step mechanism in which the target electron is first excited and in a subsequent stage effectively captured by the impinging projectile.

CONCLUSIONS

In this work, we have presented an experimental/theoretical exploration of the Ne^{8+} +Na(3s) collision system in the 1-10 keV/amu energy range. We have found evidence of oscillatory structures in state selective charge exchange cross sections which according to our CTMC analysis can be associated to the way in which the partial contributions of the 1-, 3- and 5- swap mechanisms add up at different impact energies. The recoil ion transverse momentum distributions for selected *n*-values have been also explored, finding that for $n \geq 9$ the distributions show a similar 1-peak structure while an oscillatory pattern is obtained for $n \leq 10$. We point out that electron capture to levels $n \leq 10$ is only possible via a two-step mechanism of an initial electronic excitation followed by the charge exchange itself.

ACKNOWLEDGMENTS

Work at KVI is supported by the Helmholtzzentrum für Schwerionenforschung GmbH (GSI), Germany-KVI University of Groningen collaboration agreement. Work at UNS is supported by PGI 24/F049 of UNS and PIP 112-200801-02760 of CONICET (Argentina).

REFERENCES

1. R. B. Berstein, *Molecular Beams*, New York: Interscience, 1966, pp. 75-134.
2. J. Perel, R. H. Vernon and H. L. Daley, *Phys. Rev.* **138**, A937-A946 (1965).
3. R. E. Olson, *Phys. Rev.* **187**, 153-161 (1969).
4. K. B. MacAdam, J. C. Day, J. C. Aguilar, D. M. Homan, A. D. MacKellar and N. J. Cavagnero, *Phys. Rev. Lett.* **75**, 1723-1726 (1995).
5. D. R. Schultz, C. O. Reinhold and P. S. Krstic, *Phys. Rev. Lett.* **78**, 2720-2723 (1997).
6. R. Moshammer, M. Unverzagt, W. Schmitt, J. Ullrich and H. Schmidt-Böcking, *Nucl. Instr. Meth. Phys. Res. B* **108**, 425-445 (1996).
7. X. Flechard, H. Nguygen, E. Wells, I. Ben-Itzhak and B. D. DePaola, *Phys. Rev. Lett.* **87**, 123203 (1-4) (2001).
8. M. Van der Poel, C. V. Nielsen, M. A. Gearba adn N. Andersen, *Phys. Rev. Lett.* **87**, 123201 (1-4) (2001).
9. J. M. Turkstra, R. Hoekstra, S. Knoop, D. Meyer, R. Morgenstern and R. E. Olson, *Phys. Rev. Lett.* **87**, 123202 (1-4) (2001).
10. S. Knoop, R. E. Olson, H. Ott, V. G. Hasan, R. Morgenstern and R. Hoekstra, *J. Phys. B: At. Mol. Opt. Phys.* **38**, 1987-1998 (2005).

11. S. Otranto and R. E. Olson, , *J. Phys. B: At. Mol. Opt. Phys.* **43**, 144004 (1-6) (2010).
12. S. Otranto and R. E. Olson, , *J. Phys. B: At. Mol. Opt. Phys.* **43**, 155203 (1-8) (2010).
13. S. Otranto, R. E. Olson, V. G. Hasan and R. Hoekstra, *AIP Conf. Proc.* **1336**, 158-161 (2011).
14. I. Blank, S. Otranto, C. Meinema, R. E. Olson and R. Hoekstra, *Phys. Rev. A* **85**, 022712 (1-8) (2012).
15. I. Blank, S. Otranto, C. Meinema, R. E. Olson and R. Hoekstra, *to be published.*
16. R. H. Garvey, C. H.Jackman and A. E. S. Green, *Phys. Rev. A* **12**, 1144-1152 (1975).